Available online at www.sciencedirect.com

ScienceDirect

Energy Procedia 140 (2017) 467–474

Energy Procedia

www.elsevier.com/locate/procedia

AiCARR 50th International Congress; Beyond NZEB Buildings, 10-11 May 2017, Matera, Italy

Indirect evaporative cooling systems: an experimental analysis in summer condition

Stefano De Antonellis[a,*], Cesare Maria Joppolo[a], Calogero Leone[b], Paolo Liberati[b], Samanta Milani[a]

[a]*Politecnico di Milano, Dipartimento di Energia, MI*
[b]*Recuperator S.p.A. – Rescaldina, MI*

Abstract

Indirect evaporative coolers (IEC) are components that can be effectively installed in air handling units to increase energy efficiency of air conditioning systems. In particular, such devices can be used in summer conditions to reduce chiller load in both existing and new buildings. In this paper, an IEC system based on a cross flow heat exchanger has been tested, evaluating its cooling capacity in different operating conditions. Performance is evaluated in terms of wet bulb effectiveness, primary air temperature reduction and fraction of evaporated water. Results put in evidence that a significant cooling capacity can be achieved in many operating conditions. Therefore, IECs are a promising technology that can be effectively used to reduce primary energy consumption of conventional systems.

Peer-review under responsibility of the scientific committee of the AiCARR 50th International Congress; Beyond NZEB Buildings.

Keywords: indirect evaporative cooling; performance; experimental; summer conditions;

1. Introduction

Indirect evaporative cooling is an effective technology that can be used to reduce primary energy consumption of conventional cooling systems. At present, interest in such systems is increasing to reduce chiller load in both existing and new buildings.

* Corresponding author. Tel.: +39 02 23993823;
E-mail address: stefano.deantonellis@polimi.it

1876-6102
Peer-review under responsibility of the scientific committee of the AiCARR 50th International Congress; Beyond NZEB Buildings
10.1016/j.egypro.2017.11.158

Nomenclature

$A_{HE,net}$	Heat exchanger net cross section area, m^2
f_{eva}	Fraction of evaporated water, -
h	Net channel height, m
H_{HE}	Heat exchanger height, m
L	Net heat exchanger length, m
$\dot{M}$	Mass flow rate, kg s^{-1}
N_{HE}	Number of heat exchanger plates, -
pt	Heat exchanger plates pitch, m
$\dot{Q}$	Volumetric air flow rate, m^3 h^{-1}
$\dot{Q}_w$	Volumetric water flow rate, l h^{-1}
T	Temperature, °C
v	Velocity, m s^{-1}
X	Humidity ratio, kg kg^{-1}

Superscripts

N	Reference density (ρ = 1.2 kg m^{-3})

Subscripts

a	Air
aa	Ambient (indoor) air
ea	External (outdoor) air
in	Inlet
out	Outlet
pa	Primary air
sa	Secondary air
w	Water
wb	Wet bulb

Greek symbols

δ	Heat exchanger plates thickness, mm
ΔT	Temperature difference, °C
ε	Heat exchanger effectiveness, -
ε_{wb}	Wet bulb IEC effectiveness, -
ρ	Density, kg m^{-3}
φ	Relative humidity, -

Performance of these devices strongly depends on constructive and operating parameters, such as heat exchanger technical specifications, primary and secondary air conditions and water flow rate. At present, many research works deal with the development of this technology, both through a numerical and experimental approach. Several authors analysed performance of different prototypes [1,2], the effect of different operating conditions [3-5] and system orientation [6,7]

In this work a detailed experimental analysis of an indirect evaporative cooling system is discussed. Inlet temperature and relative humidity of both air streams are set to be representative of summer operating conditions in residential and commercial applications. It is assumed that the secondary air stream is the exhaust air flow from the building and the primary air stream is at outdoor conditions.

2. Experimental setup

The investigated indirect evaporative cooling system consists of the following components, as shown in Figure 1:

- A cross flow plate heat exchanger.
- N° 8 water nozzles installed in the secondary air inlet plenum.
- A system to increase pressure of water supplied to nozzles.

The heat exchanger is made of aluminium plates with semispherical dimples. Hereinafter main characteristics of the device are reported:

- Plates orientation: vertical.
- N° of plates N_{HE} = 119.
- Plates thickness δ = 0.14 mm.
- Plates pitch pt = 3.35 mm.
- Net channel height $h = pt - \delta$ = 3.21 mm.
- Net plate length and width L = 485 mm.

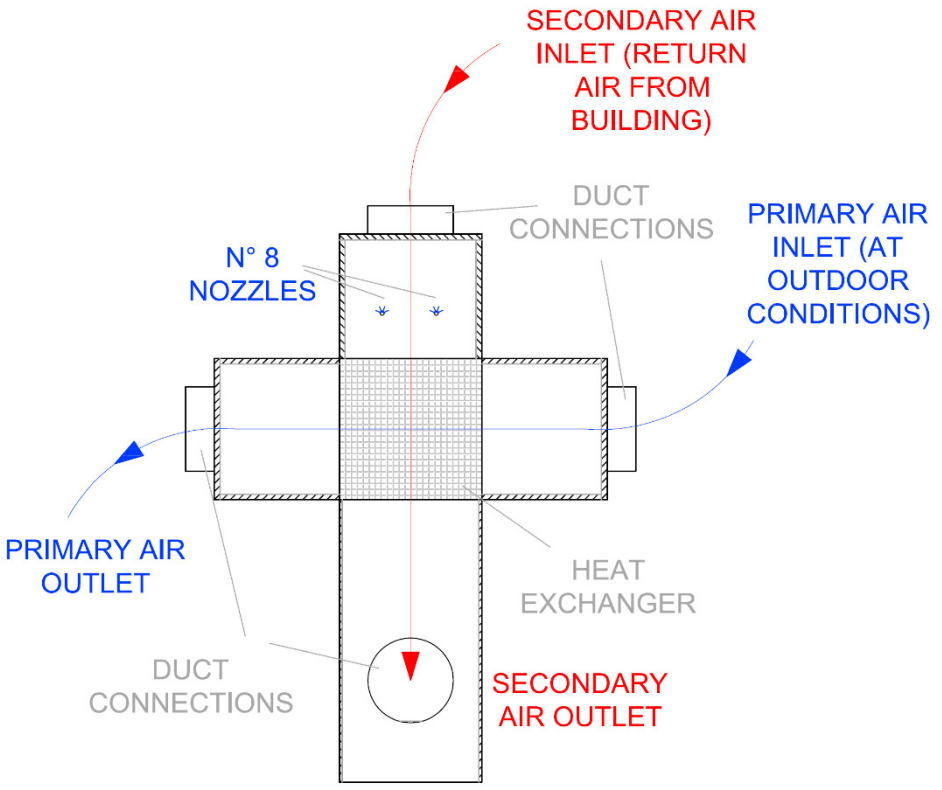

Fig. 1. Scheme of the experimental setup

It is highlighted that in case of balanced air flows, with air velocity v_a^N=3.2 m s^{-1} at reference conditions (ρ_a^N=1.2 kg m^{-3}), the heat exchanger effectiveness, defined as $\varepsilon = \dot{M}_{pa}\, cp_{pa}\, (T_{pa,in} - T_{pa,out}) / [(\dot{M}_a\, cp_a)_{\min}\, (T_{pa,in} - T_{sa,in})]$ is equal to 0.625. In that conditions and at T_a= 35°C, the pressure drop is around 100 Pa.

Water nozzles are installed on two parallel manifolds (n° 4 nozzles on each manifold): the distance between each of them is around 8 cm. Instead, each manifold is 15 cm far from the heat exchanger face and the distance between the two manifolds is around 18 cm.

According to Fig. 1, the secondary air stream flows from the top to the bottom of the system. Nozzles are installed in the top plenum (secondary air inlet), supplying water in counter current arrangement respect to the air stream. The primary air stream crosses the heat exchanger from the right to the left.

Length of top and side plenums is 42 cm, length of bottom one is 90 cm.

The nominal water flow rate of each axial flow - full cone nozzle is 7.50 l h^{-1} at 9 bar (data provided by the manufacturer).

The net cross section area of the heat exchanger is equal to 0.089 m^2, being calculated in the following way:

$$A_{HE,net} = \frac{\left(H_{HE} - N_{HE}\,\delta\right) L}{2} \tag{1}$$

Where the net heat exchanger height is:

$$H_{HE} = \left(N_{HE} - 1\right) pt + \delta \tag{2}$$

Inlet primary and secondary air conditions (temperature, humidity ratio and flow rate) are set through two independent air handling units. A detailed description of the experimental setup has been reported in previous works of the authors [5,8].

Temperature and relative humidity are measured at the inlet and outlet of the investigated system through RTD PT100 sensors (±0.2°C at 20°C) coupled to capacitive relative humidity sensors (± 1% between 0 and 90%).

3. Methodology

In this research work n°40 experimental tests have been performed, in order to evaluate performance of the system, as summarized in Table 1. It is assumed that:

- Inlet primary air is at outdoor summer air conditions: $T_{pa,in} = T_{ea}$ = 30 °C or 35 °C and $\varphi_{pa,in} = \varphi_{ea}$ = 40 %.
- Inlet secondary air is at indoor air conditions (return air stream from the building): $T_{sa,in} = T_{aa}$ = 24 °C or 26 °C and $\varphi_{sa,in} = \varphi_{aa}$ = 60 %.
- Primary air flow rate $\dot{Q}_{pa}^N$ is equal to 1200 m^3 h^{-1} at reference conditions.
- Secondary air flow rate $\dot{Q}_{sa}^N$ is set equal to $\dot{Q}_{pa}^N$ (1200 m^3 h^{-1}) or equal to 80% of $\dot{Q}_{pa}^N$ (960 m^3 h^{-1}). The second case is representative of actual applications where the return air stream from the building is smaller than the supply one.

The water has been supplied to the secondary air stream in the top plenum at a temperature around 20°C. The water flow has been varied between $\dot{Q}_{w,in}$ = 30 l h^{-1} and $\dot{Q}_{w,in}$ = 65 l h^{-1}.

In each test session, experimental data have been collected in steady state conditions at a frequency of 1 Hz (300 samples of each physical quantity). Experimental uncertainty of direct monitored variable has been calculated according to international standards [9].

Table 1. Experimental test conditions adopted in the present study

Test [-]	$T_{pa,in}$ [°C]	$\varphi_{pa,in}$ [%]	$\dot{Q}_{pa}^{N}$ [m^3 h^{-1}]	$T_{sa,in}$ [°C]	$\varphi_{sa,in}$ [%]	$\dot{Q}_{sa}^{N}$ [m^3 h^{-1}]	$\dot{Q}_{w,in}$ [l h^{-1}]
1	30	40	1200	24	60	1200	30-65
2	35	40	1200	24	60	1200	30-65
3	30	40	1200	26	60	1200	30-65
4	35	40	1200	26	60	1200	30-65
5	30	40	1200	24	60	960	30-65
6	35	40	1200	24	60	960	30-65
7	30	40	1200	26	60	960	30-65
8	35	40	1200	26	60	960	30-65

Comparison between experimental data has been performed in terms of wet bulb effectiveness, primary air temperature difference and fraction of evaporated water. Such quantities are defined in the following way:

$$\varepsilon_{wb} = \frac{T_{pa,in} - T_{pa,out}}{T_{pa,in} - T_{wb,sa,in}} \tag{3}$$

$$\Delta T_{pa} = T_{pa,in} - T_{pa,out} \tag{4}$$

$$f_{eva} = \frac{\dot{Q}_{sa}^{N} \rho_{a}^{N} \left(X_{sa,out} - X_{sa,in} \right)}{\dot{M}_{w,in} 3600} \tag{5}$$

Where $\dot{M}_{w,in}$ is the inlet water mass flow rate.

4. Results analysis

In Fig. 2 it is shown the comparison A, between experimental tests 1 and 2 (Tab. 1). Primary air inlet temperature $T_{pa,in}$ (equal to T_{ea}) is set equal to 30°C or 35°C. The wet bulb effectiveness ε_{wb} (in Fig. 2 - A1), expressed as a function of volumetric water flow rate $\dot{Q}_{w,in}$, varies slightly at different external air temperatures in summer conditions. The effectiveness remains roughly constant due to a comparable variation in numerator (temperature difference of primary air) and denominator of equation (3).

Moreover, an increase in the water flow rate always leads to an increase in the wet bulb effectiveness, as shown in a previous analysis [5]. In fact, the higher the water flow rate, the higher the wet fraction of heat exchanger surface and, therefore, the water evaporation rate.

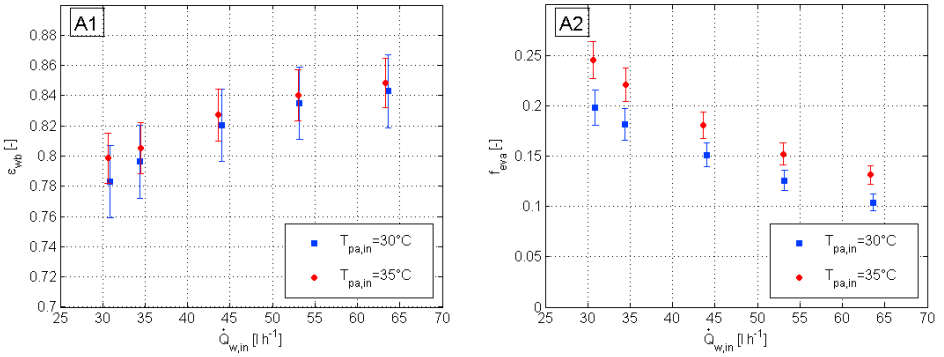

Fig. 2. Comparison A between tests 1 and 2 (secondary air flow rate $\dot{Q}_{sa}^{N}$ equal to 1200 m^3 h^{-1}, secondary air temperature equal to 24°C). Wet bulb effectiveness ε_{wb} (figure A1) and fraction of evaporated water f_{eva} (Figure A2) as a function of volumetric water flow rate $\dot{Q}_{w,in}$.

The fraction of evaporated water f_{eva} decreases as inlet water flow rate increases (Fig. 2 - A2): in fact, in this test condition only part of the additional water supplied to the system evaporates. Finally, the higher the primary air inlet temperature, the higher f_{eva} due to the higher plates temperature.

In Fig. 3, it is shown the comparison B, between experimental tests 3 and 4 (Tab. 1), where the primary air inlet temperature has been set equal to 26°C. The wet bulb effectiveness ε_{wb} (Fig. 3 - B1) increases as water flow rate increases and, also in this case, it does not change significantly with primary air temperature. The fraction of evaporated water f_{eva} (Fig. 3 - B2) is higher when primary air temperature is equal to 35 °C.

Comparing results of Fig. 2 with ones of Fig. 3, it is possible to state that in the investigated tests the variation of the secondary air inlet conditions has limited effect on ε_{wb} and f_{eva}. In fact, in both cases the difference $T_{sa,in} - T_{wb,sa,in}$ is almost constant.

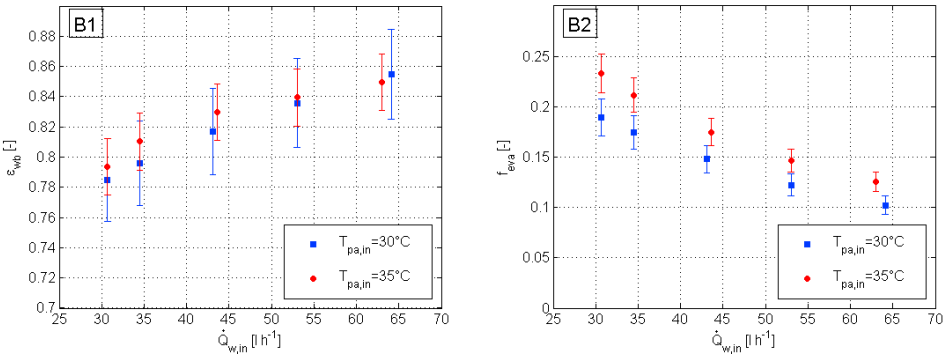

Fig. 3. Comparison B between tests 3 and 4 (secondary air flow rate $\dot{Q}_{sa}^{N}$ equal to 1200 m^3 h^{-1}, secondary air temperature equal to 26°C). Wet bulb effectiveness ε_{wb} (figure B1) and fraction of evaporated water f_{eva} (Figure B2) as a function of volumetric water flow rate $\dot{Q}_{w,in}$.

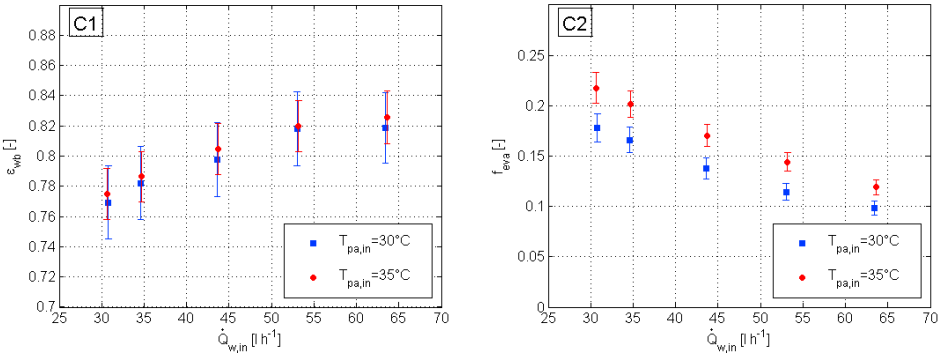

Fig. 4. Comparison C between tests 5 and 6 (secondary air flow rate $\dot{Q}_{sa}^{N}$ equal to 960 m^3 h^{-1}, secondary air temperature equal to 24°C). Wet bulb effectiveness ε_{wb} (figure C1) and fraction of evaporated water f_{eva} (Figure C2) as a function of volumetric water flow rate $\dot{Q}_{w,in}$.

In Fig. 4 and Fig. 5 the comparisons between tests 5-6 ($T_{sa,in}$ = 24°C) and 7-8 ($T_{sa,in}$ = 26°C) are respectively shown. In these tests the secondary air flow rate is set equal to 960 m^3 h^{-1}. As previously reported, such test conditions are representative of applications where return air flow from the building is lower than the supply one. The wet bulb effectiveness and the fraction of evaporated water trends are slightly affected by the secondary air flow rate variation. The lower $\dot{Q}_{sa}^{N}$, the lower ε_{wb} and f_{eva} due to the reduced amount of water evaporation.

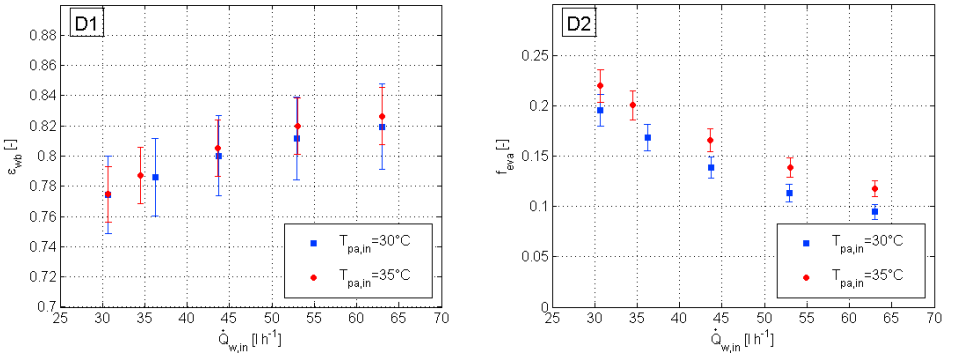

Fig. 5. Comparison D between tests 7 and 8 (secondary air flow rate $\dot{Q}_{sa}{}^{N}$ equal to 960 m^3 h^{-1}, secondary air temperature equal to 26°C). Wet bulb effectiveness ε_{wb} (figure D1) and fraction of evaporated water f_{eva} (Figure D2) as a function of volumetric water flow rate $\dot{Q}_{w,in}$.

Fig. 6 shows the primary air temperature difference ΔT_{pa}, which is a direct index of cooling capacity, in tests 1, 2, 3, and 4 ($\dot{Q}_{sa}{}^{N}$ = 1200 m^3 h^{-1}). Quite obviously, a higher primary air inlet temperature leads to a higher cooling effect on primary airflow. Instead, although it has been discussed that in the investigated tests ε_{wb} slightly depends on secondary air conditions, ΔT_{pa} decreases by increasing $T_{sa,in}$ (at constant $\varphi_{sa,in}$).

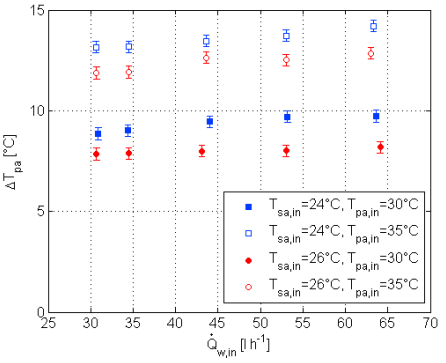

Fig. 6. Primary air temperature difference ΔT_{pa} as a function of volumetric water flow rate $\dot{Q}_{w,in}$. Comparison between tests 1,2,3, and 4 (secondary air flow rate $\dot{Q}_{sa}{}^{N}$ equal to 1200 m^3 h^{-1}).

5. Conclusions

In this work an experimental analysis of a IEC system in summer conditions has been performed. The investigation deals with the variation of primary air inlet temperature, secondary air flow rate and water flow rate.

Most significant results are:

- An increase in outside air temperature (primary air inlet temperature) slightly influences the wet bulb effectiveness.
- A variation of indoor air condition (secondary air inlet condition) slightly influences the wet bulb effectiveness and the fraction of evaporated water.
- A reduction in the return air stream rate (secondary air stream) leads to a slight reduction in the wet bulb effectiveness.
- Depending on inlet air conditions, the reduction of supply air temperature varies between 8°C and 14°C.

Based on results of this study, it is possible to state that the IEC technology can provide a significant contribution to increase conventional HVAC system efficiency when operating in summer conditions.

References

[1] Bruno F. 2011. On-site experimental testing of a novel dew point evaporative cooler. Energy and Buildings, 43 (12), 3475-3483
[2] Tejero-González A., Andrés-Chicote M., Velasco-Gómez E., Rey-Martínez F.J. 2013. Influence of constructive parameters on the performance of two indirect evaporative cooler prototypes. Applied Thermal Engineering, 51 (1-2), 1017-1025
[3] Heidarinejad G., Bozorgmehr M., Delfani S., Esmaeelian J. 2009. Experimental investigation of two-stage indirect/direct evaporative cooling system in various climatic conditions. Building and Environment 44 (10) 2073-2079
[4] Kim M.-H., Kim J.-H., Choi A.-S., Jeong J.-W. 2011. Experimental study on the heat exchange effectiveness of a dry coil indirect evaporation cooler under various operating conditions. Energy, 36 (11), 6479-6489
[5] De Antonellis S., Joppolo C.M., Liberati P., Milani S., Molinaroli L. 2016. Experimental analysis of a cross flow indirect evaporative cooling system. Energy and Buildings, 121, 130-138
[6] De Antonellis S., Joppolo C.M., Liberati P., Milani S. 2016. Analisi sperimentale delle prestazioni di un sistema di raffreddamento evaporativo indiretto. 34° Convegno Nazionale AICARR. Bologna (Italy), 20/10/2016.
[7] Saman W.Y., Alizadeh S. 2002. An experimental study of a cross-flow type plate heat exchanger for dehumidification/cooling. Solar Energy, 73 (1), 59-71
[8] De Antonellis S., Intini M., Joppolo C.M., Molinaroli L., Romano F. 2015. Desiccant wheels for air humidification: An experimental and numerical analysis. Energy Conversion and Management, 106, 355-364
[9] JCGM. 2008. Evaluation of measurement data – Guide to the expression of uncertainty in measurement JCGM 100 (GUM 1995 with minor corrections)